



Epididymal Fat-Derived Sympathoexcitatory Signals Exacerbate Neurogenic Hypertension in Obese Male Mice Exposed to Early Life Stress

Carolina Dalmasso, Jacqueline R. Leachman, Sundus Ghuneim, Nermin Ahmed, Eve R. Schneider^{id}, Olivier Thibault, Jeffrey L. Osborn, Analia S. Loria^{id}

ABSTRACT: Previously, we have shown that male mice exposed to maternal separation and early weaning (MSEW)—a mouse model of early life stress—display increased mean arterial pressure compared with controls when fed a high-fat diet. As the stimulation of sensory nerves from fat has been shown to trigger the adipose afferent reflex, we tested whether MSEW male mice show obesity-associated hypertension via the hyperactivation of this sympathoexcitatory mechanism. After 16 weeks on high-fat diet, MSEW mice displayed increased blood pressure, sympathetic activation, and greater depressor response to an α -adrenergic blocker when compared with controls ($P<0.05$; $n=8$), despite no differences in adiposity and plasma leptin. The acute infusion of capsaicin in epididymal white adipose tissue (1.5 pmol/ μ L of capsaicin, 8 μ L/per site, 4 sites, bilaterally) increased the total pressor response in MSEW mice compared with controls (110 \pm 19 versus 284 \pm 33 mm Hg \times 30 minutes; $P<0.05$; $n=8$). This response was associated with neuronal activation in OVLT, posterior paraventricular nucleus of the hypothalamus, and RVLM ($P<0.05$ versus control; $n=6-7$). Renal denervation abolished both the acute and chronic elevated mean arterial pressure in obese MSEW mice. Moreover, selective sensory denervation of epididymal white adipose tissue using resiniferatoxin (10 pmol/ μ L solution; $n=6$) decreased mean arterial pressure in obese MSEW mice only ($P<0.05$ versus control). Obese MSEW mice displayed increased epididymal white adipose tissue levels of both tryptophan hydroxylase (Tph1) mRNA expression and its synthesis product serotonin (8.3 \pm 1.9 versus 16.6 \pm 1.7 μ g/mg tissue; $P<0.05$ versus control). Thus, afferent sensory signals from epididymal white adipose tissue may contribute to the exacerbated fat-brain-blood pressure axis displayed by obese male mice exposed to early life stress. (*Hypertension*. 2021;78:1434–1449. DOI: 10.1161/HYPERTENSIONAHA.121.17298.) • [Data Supplement](#)

Key Words: adiposity ■ blood pressure ■ capsaicin ■ leptin ■ serotonin

Obesity is one of the major risk factors for hypertension and cardiovascular disease affecting \approx 40% of Americans.^{1,2} In just 2 decades (1999–2018), the prevalence of obesity increased from 30.5% to 42.4%, unveiling the uncontrolled status of this epidemic.² Obesity-related conditions including heart disease, hypertension, and type 2 diabetes are some of the leading causes of preventable, premature death. Among adults, the prevalence of obesity is the highest among non-Hispanic Blacks and Hispanics,² suggesting that

groups with health disparities and disadvantaged populations may be at higher risk. Thus, an unhealthy diet combined with genetics and psychosocial factors could favor the development of comorbidities such as obesity and hypertension.

The overactivation of the sympathetic nervous system (SNS) is one of the most studied mechanisms underlying the development of obesity-induced hypertension.^{3–6} The fat-derived hormone leptin has been shown to increase energy expenditure and enhance the sympathetic drive

Correspondence to: Analia S. Loria, Department of Pharmacology and Nutritional Sciences, University of Kentucky, 900 S Limestone St, 562 Charles T Wethington Bldg, Lexington, KY 40536. Email analia.loria@uky.edu

The Data Supplement is available with this article at <https://www.ahajournals.org/doi/suppl/10.1161/HYPERTENSIONAHA.121.17298>.

For Sources of Funding and Disclosures, see page 1446.

© 2021 The Authors. *Hypertension* is published on behalf of the American Heart Association, Inc., by Wolters Kluwer Health, Inc. This is an open access article under the terms of the [Creative Commons Attribution Non-Commercial-NoDerivs](#) License, which permits use, distribution, and reproduction in any medium, provided that the original work is properly cited, the use is noncommercial, and no modifications or adaptations are made.

Hypertension is available at www.ahajournals.org/journal/hyp

Novelty and Significance

What Is New?

- The study of the fat–brain–blood pressure axis mediating obesity associated hypertension in a model of early life stress.
- The use of selective afferent denervation of the adipose tissue to attenuate blood pressure.
- The identification of serotonin as an endogenous factor that may contribute to the stimulation of the afferent sensory neurons.

What Is Relevant?

- Early life stress exacerbates afferent signals from visceral white adipose tissue, which increases neuronal activation in brain areas that contribute to blood pressure regulation by mediating sympathetic outflow to the kidneys of obese male mice.

- As obesity increases the risk of drug-resistant hypertension, identifying novel contributors enhancing sympathetic activation is critical in developing more specific therapeutic approaches. This will be of particular importance for the successful management of hypertension associated with obesity in patients affected by nontraditional risk factors.

Summary

This study demonstrates that afferent signals from visceral white adipose tissue contribute to the sympathetic drive activation and hypertension in male mice exposed to early life stress when fed an obesogenic diet. This enhanced sympathetic outflow is most likely mediated by increased afferent signals from epididymal white adipose tissue projecting to brain areas with a pivotal role developing neurogenic hypertension.

Nonstandard Abbreviations and Acronyms

AAR	adipose afferent reflex
eWAT	epididymal white adipose tissue
FG	FluoroGold
HF	high fat diet
HR	heart rate
Lepr	leptin receptor
LF	low fat diet
MAP	mean arterial pressure
MSEW	maternal separation and early weaning
PD	postnatal day
PVN	paraventricular nucleus of the hypothalamus
RSNA	renal sympathetic nerve activity
RTX	resiniferatoxin
Tph1	tryptophan hydroxylase 1
TRPA1	transient receptor potential cation channel, subfamily A, member 1
TRPV1	transient receptor potential cation channel, subfamily V, member 1
WAT	white adipose tissue

to key organs implicated in blood pressure regulation, such as the kidney.^{7–10} However, experimental studies have demonstrated that afferent signals from white adipose tissue (WAT) can also influence blood pressure through a sympathoexcitatory mechanism known as the adipose afferent reflex (AAR).^{11–13} Under physiological

conditions, the activation of the AAR prevents fat deposition by inducing lipolysis and lipid mobilization in WAT and promoting leptin release.^{14–17} However, pathophysiological conditions with metabolic compromise such as obesity and diabetes result in the overactivation of the AAR, contributing to increases in the SNS outflow and blood pressure. Xiong et al^{11,18} reported that the experimental stimulation of the AAR in inguinal WAT using capsaicin—a TRPV1 (transient receptor potential cation channel subfamily V member 1) ligand that activates sensory neurons—increased blood pressure in rats undergoing diet-induced obesity and hypertension. Acute AAR stimulation increased both the fat afferent nerve activity, the renal sympathetic nerve activity (RSNA), and correlated with increased neuronal activation in the paraventricular nucleus of the hypothalamus (PVN).^{11,19} Furthermore, the selective ablation of adipose tissue sensory neurons reduced RSNA and blood pressure. In previous work from the same group, the authors demonstrated that the AAR could also be stimulated by WAT infusions of bradykinin, adenosine, or leptin, resulting in increased RSNA and mean arterial pressure (MAP) in normotensive rats.¹⁸ Moreover, bilateral infusions of a leptin antagonist in inguinal and retroperitoneal WAT in obese hypertensive rats were able to decrease the RSNA and MAP.¹¹

Recently, our laboratory has demonstrated, for the first time in mice, that the stimulation of sensory neurons from WAT can increase blood pressure similarly to what has been reported in rats.²⁰ In addition, we showed that the AAR stimulation of subcutaneous WAT with capsaicin did not induce any hemodynamic effect, whereas the epididymal WAT (eWAT) stimulation increased blood

pressure.²⁰ These findings are in line with numerous studies demonstrating the contribution of visceral adiposity to increased blood pressure during obesity.³

Early life stress is defined as any form of abuse, neglect, or loss during the first decade of life, promoting long-lasting effects on physiological and mental function, increasing the overall risk for chronic disease.²¹ Epidemiological studies have established early life stress as an independent risk factor associated with increased body mass index and blood pressure, contributing to the development of hypertension and cardiovascular disease.^{22–25} Postnatal maternal separation and early weaning (MSEW) is an experimental mouse model that recapitulates several aspects of the impact of early life stress on the cardiovascular and metabolic system.^{26–28} Previous studies from our laboratory have shown that male mice exposed to MSEW and fed a high fat diet (HF) display significantly increased blood pressure compared with controls.²⁸ However, the mechanism by which MSEW exacerbates blood pressure sensitivity is not completely understood.

The fact that the maternal separation paradigm induces neuronal activation in PVN^{29–32} supports the notion that the AAR mechanism could be sensitized in response to acute or chronic stimuli in which the PVN plays a pivotal role. Therefore, this study tested the hypothesis that exacerbated AAR contributes to the development of obesity-induced hypertension in MSEW male mice compared with controls. We assessed the AAR function at 3 different levels: (1) we investigated the effects of capsaicin on the acute blood pressure response and on the neuronal activation in different brain areas and whether the changes in blood pressure are mediated by the renal nerves, (2) we tested whether the selective ablation of afferent sensory neurons innervating eWAT lowered blood pressure, and (3) we determined the eWAT gene expression of key factors known to stimulate sensory neurons, looking for endogenous ligands that may exacerbate the AAR in obese MSEW male mice.

METHODS

The data that support the findings of this study are available from the corresponding author upon reasonable request.

Animals

All experiments followed the National Institutes of Health Guide for the Care and Use of Laboratory Animals and were approved and monitored by the Institutional Animal Care and Use Committee at the University of Kentucky. C57BL/6 female and male mice (The Jackson Laboratory, East Division) used for breeding had ad libitum access to food and water and were housed in a pathogen-free environment with constant temperature and humidity, with a 14:10-hour light:dark cycle. Animals were fed a regular chow diet (Teklad 8604; Madison, WI).

MSEW was conducted as described previously.²⁸ Briefly, culled litters (6–8 pups) were separated from the dams and transferred to a clean cage in an incubator (30±1 °C; humidity, 60%) for 4 hours from postnatal day (PD) 2 to PD 5 and for 8 hours from PD 6 to PD 16. Early weaning was performed at PD 17. Normally reared, nonhandled litters that remained with the dams served as control groups and were weaned at PD 21. Male littermates were randomized at weaning and used for the experiments outlined in this study, whereas female littermates were used for other projects. Only one mouse per litter was used in each experiment.

Experimental Design

Detailed *in vivo* procedures, staining, and imaging techniques can be found in the [Data Supplement](#). At weaning, MSEW and control male mice were randomly placed for 16 weeks on a low fat diet (LF, 10% kcal from fat, D12450J; Research Diets, New Brunswick, NJ) or HF (60% kcal from fat, D12492; Research Diets). Then, body composition was measured using an Echo magnetic resonance imaging system (Echo Medical Systems, Houston, TX). A subset of mice (n=8 per group) was used to perform an *in vivo* lipolysis assay by injecting sterile saline or CL-316,243 hydrate (50 µL, 1 mg/kg, intraperitoneal [IP] injection). After 1 hour, a submandibular blood sample was collected. A week later, mice were euthanized for blood collection to measure plasma leptin by ELISA (Cayman Chemical, Ann Arbor, MI), following the manufacturer's protocol. Aliquots of eWAT were snap-frozen to determine gene and protein expression or incubated in DMEM +2% FFA-BSA (50 mg/250 µL, 1 hour, 37 °C) to measure eWAT-derived leptin. Another aliquot of eWAT (≈100 mg) was incubated with HEPES-KRH buffer (125 mmol/L NaCl, 5 mmol/L KCl, 1.8 mmol/L CaCl₂, 2.6 mmol/L MgSO₄, 5 mmol/L HEPES, pH 7.2) in the presence of saline or isoproterenol (10 µM, 1 hour) to determine *in vivo* lipolysis. Glycerol levels in plasma and KRH media explant in response to lipolysis tests were measured by ELISA (≈1:8 dilution; Cayman Chemical, Ann Arbor, MI).

Acute Hemodynamic Measurements to Assess Sympathetic Activation

After 15 weeks on HF, mice were subjected to a transcutaneous glomerular filtration rate measurement as described previously.³³ Then, mice were implanted with radiotelemeters (TAA11PA-C10; Data Sciences International, New Brighton, MN). After a 10-day recovery period, systolic, diastolic, MAP, and heart rate (HR) baselines were measured for 5 consecutive days in a 10-second sampling period, recorded and averaged every 5 minutes. Then, the response to prazosin (1 mg/kg, IP; Sigma-Aldrich, St. Louis, MO), mecamylamine (5 mg/kg, IP; Sigma-Aldrich), propranolol (5 mg/kg, IP; Sigma-Aldrich), and atropine (1 mg/kg, IP; Sigma-Aldrich) was assessed allowing full recovery between the different treatments. To determine the effects on blood pressure and HR, a 5-minute average was analyzed for 2 hours before and 6 hours after each injection. In a subset of mice, bilateral renal denervation (RNDX) was performed to determine its effect on baseline MAP. Renal cortical norepinephrine content was measured by ELISA (BA E-5200R; Rocky Mountain Diagnostic, Inc, Colorado Springs,

CO) in RDNX and in control surgery for RDNX (Sham) renal cortexes homogenized in metabisulfite buffer (1 mmol/L EDTA and 4 mmol/L metabisulfite in 0.01 N HCl, 1:100 dilution Sham, 1:20 dilution RDNX) as described previously.³⁴

Fat–Brain–Blood Pressure Axis Evaluation via the Acute AAR Stimulation

In a set of control and MSEW mice fed LF or HF for 16 weeks, carotid catheters were implanted under isoflurane anesthesia for MAP measurements (Power Lab; ADInstruments, CO) in response to the acute stimulation of the AAR in subcutaneous or eWAT with vehicle or capsaicin as described previously.²⁰ Subcutaneous WAT or eWAT depots were exposed and 4 thin and sharp stainless steel needles (0.31 mm outer diameter; 4 mm apart) were inserted into the fat pad bilaterally (3 mm below the surface). The needles were connected with PE-10 tubes to an infusion pump (PHD Ultra Harvard Apparatus, MA). The AAR was induced by the infusion of vehicle (20 μ L ethanol, 10 μ L tween 80/mL normal saline) or 1.5 pmol/ μ L of capsaicin (8 μ L capsaicin solution over a period of 2 minutes in 4 different sites, bilaterally). Capsaicin solution consisted of 5 ng capsaicin (M2028; Sigma-Aldrich), 20 μ L ethanol, and 10 μ L tween 80/mL normal saline. Baseline MAP was recorded for 20 minutes. Next, blood pressure was recorded in response to vehicle or capsaicin for another 30 minutes. After stimulation, animals were euthanized.

The total pressor area under the curve was calculated using a 20-minute recording prior to the stimulation as a baseline, as reported previously.³⁵ In a second set of mice, bilateral RDNX (10% phenol in alcohol solution) was performed 4 days before the acute response to capsaicin, to determine the role of the renal nerves on blood pressure response to eWAT stimulation. Blood pressure response was measured continuously and averaged every 30 seconds for 30 minutes. Sham surgery for RDNX was conducted by carefully exposing the renal nerves, painting them with normal saline and closing the muscle and skin. In a third set of mice, neuronal activation was evaluated using c-Fos, a marker of neuronal activation, combined with the retrograde fluorescent tracer FluoroGold (FG; 40 mg/kg, IP; Fluorochrome, Denver, CO) FG only labels neuroendocrine neurons in the brain that receive projections from areas that are in direct contact with fenestrated capillaries, since it does not cross the blood-brain barrier.³⁶ Neuroendocrine neurons are positive for both FG and c-Fos, while nonendocrine neurons, for example, the parvocellular nonendocrine neurons in PVN, are positive only for c-Fos. Five days after FG injection, mice were euthanized, and brains were fixed with 4% paraformaldehyde to determine Fos immunoreactivity (1:4000, RPCA-c-FOS; EnCor Biotechnology, FL).

Sensory Denervation of eWAT

After a 5-day baseline MAP measurement, mice implanted with radiotelemetry were injected with vehicle in eWAT (SHAM). Under isoflurane anesthesia, epididymal fat depots were exposed through a 1-cm incision to the left of the abdominal midline. Sharp stainless steel needles were inserted following the procedure described for capsaicin infusion. First, mice were infused with vehicle (0.6% ethanol in normal saline; 4 μ L per site; 8 sites; bilateral), and blood pressure was recorded for 4

consecutive days. In a second surgery, with the incision performed to the right of the midline, mice were denervated using RTX following the same infusion protocol. RTX stock solution was prepared to a final concentration of 10 pmol/ μ L in normal saline (4 μ L RTX solution per site; 8 sites; bilateral). After 2 days, the mecamlamine response was repeated. The eWAT denervation procedure was validated using male mice with a GFP reporter in CGRP+ sensory neurons,^{37,38} B6.129P2(Cg)-Calca^{tm1.1(EGFP/HBEGF)Mjz/Mmnc} (Calca; stock number: 036773-UNC; citation ID: RRID:MMRRC_036773-UNC) as detailed in the [Data Supplement](#).

Gene Expression in eWAT

Frozen tissue (n=5–8 per group) was used to extract mRNA as reported previously.²⁸ A custom-designed Real Time quantitative Reverse Transcription Polymerase Chain Reaction (RT-qPCR) array (Bio-Rad PrimePCR; Bio-Rad Laboratories, Inc) included the following targets: Tph1 (tryptophan hydroxylase 1), Htr2a (hydroxytryptamine [serotonin] receptor 2A), TrpV1, Ngf (nerve growth factor), Bdkrb1 (bradykinin receptor, beta 1), Bdkrb2 (bradykinin receptor, beta 2), NOX4 (NADPH oxidase 4), p47phox, Ilb1 (interleukin 1 beta), Tnf (tumor necrosis factor), Lepr (leptin receptor), Cybb (cytochrome b-245, beta polypeptide), Ptgs2 (prostaglandin-endoperoxide synthase 2), Cy2c44 (cytochrome P450-family 2, subfamily c-polypeptide 44), VEGFa (vascular endothelial growth factor A), Trpa1 (transient receptor potential cation channel, subfamily A, member 1), and IL17 (interleukin 17). GAPDH was used as a housekeeper gene. Arrays were run in a Bio Rad CFX96 Touch, and data were analyzed using the Maestro software (CFX Maestro 2.0 Software; Bio-Rad Laboratories, Inc).

Serotonin Concentration in Tissue

Frozen eWAT was homogenized in cold ELISA buffer (\approx 200 mg/500 μ L), centrifuged (30 minutes, 8000 rpm, 4°C) and diluted 1:2 to perform the analysis following the manufacturer's specifications (ADI-900-175; Enzo Life Sciences, CA).

Statistical Analysis

All data are presented as mean \pm SEM. Two-way ANOVA followed by the Tukey post hoc test was used to assess the differences between control and MSEW mice in different dietary conditions. Comparisons between 2 observations in the same animal were assessed by the Student paired *t* test. One-way ANOVA repeated measures followed by Tukey was used to analyze progressive changes in MAP. In vivo and ex vivo glycerol concentration in plasma and eWAT explants was analyzed by 3-way ANOVA followed by the Tukey post hoc test. Analyses were performed using the GraphPad Software, version 9.0.0 (La Jolla, CA; www.graphpad.com). Statistical significance was determined by $P < 0.05$.

RESULTS

Body Composition and Lipolysis In Vivo and Ex Vivo

Although there was a main effect of diet on body weight, fat mass, and lean mass; MSEW showed similar body

composition compared with controls (Table). There was a main effect of MSEW on body weight; however, the adiposity was not different between groups. Accordingly, plasma and eWAT-derived media explant leptin were similar in control and MSEW, lean and obese mice (Table).

In vivo lipolysis assessment showed that HF increased the basal glycerol levels in plasma, while the response to CL-316,243 was not different between groups in either diet (Table S1 in the [Data Supplement](#)). Ex vivo lipolysis assay showed that glycerol levels at baseline were similar in all groups regardless of diet, and the stimulated lipolysis with isoproterenol increased glycerol concentration similarly in media eWAT explants from control and MSEW mice; however, media glycerol was reduced in explants from mice fed a HF compared with LF (Table S1). The 3-way ANOVA analysis showed no interaction between diet, stimulation, and MSEW factors (Figure S1).

Blood Pressure and Autonomic Function in Obese Mice

MSEW did not influence the hemodynamic parameters in mice fed a LF. However, HF-induced increases in MAP and systolic blood pressure were significant in MSEW compared with controls, while changes in diastolic blood pressure and HR were similar between groups (Table). Although obese MSEW mice showed a $\approx 20\%$ reduction

in the glomerular filtration rate, there was no significant interaction between MSEW and diet (Table).

To further investigate the origins of the exacerbated blood pressure in obese MSEW mice, we tested the autonomic status at baseline in both groups. Overall, no differences were observed between MSEW and control mice fed a LF. As shown in the Table, HF-fed MSEW mice displayed greater mecamylamine-induced decrease in MAP and propranolol-induced reduction in HR. Prazosin—an α -1 adrenergic receptor blocker—significantly decreased MAP further in MSEW males compared with controls (Table). Moreover, the decrease in MAP in response to prazosin was greater compared with the reduction induced by mecamylamine in HF-fed MSEW mice, which suggests a contribution of the vascular bed in the increased blood pressure in male MSEW mice. Finally, the blood pressure response to atropine-induced blockade of parasympathetic tone was similar in control and MSEW mice (Table). Figure S2 shows the 4-hour time course for each experiment. Table S2 shows the absolute MAP or HR changes in response to the autonomic function's evaluation.

Acute AAR Stimulation With Capsaicin

In mice fed a LF, vehicle infusions in eWAT did not change MAP in control and MSEW mice (Figure 1A),

Table. Effect of MSEW on Body Composition, Plasma and Tissue Leptin, Blood Pressure, Glomerular Filtration Rate, and Autonomic Function, in Mice Fed an LF or HF

	Control-LF	MSEW-LF	Control-HF	MSEW-HF	P^{diet}	P^{MSEW}	P^{int}
Body composition (n=22 LF, n=22 HF)							
Body weight (BW), g	28.37±0.63	29.20±0.49	45.93±0.74	48.15±0.56	<0.0001	0.152	0.260
Fat mass, %BW	11.95±0.90	13.20±1.09	37.38±0.67	38.39±0.63	<0.0001	0.183	0.890
Lean mass, %BW	84.92±0.80	83.56±1.00	59.95±0.59	59.33±0.58	<0.0001	0.233	0.643
Leptin (n=8 LF, n=8 HF)							
Plasma, ng/mL	22.66±2.77	21.38±1.88	104.51±6.84	102.84±6.05	<0.0001	0.778	0.970
eWAT, ng/mg tissue	64.60±4.97	59.26±10.21	110.66±16.05	115.04±6.95	<0.0001	0.965	0.663
Hemodynamics (n=8–9 LF, n=10 HF)							
MAP, mm Hg	108±3	109±4	110±5	120±4*†	0.004	0.024	0.048
Systolic, mm Hg	124±5	125±6	128±2	137±1*†	0.002	0.040	0.056
Diastolic, mm Hg	98±12	95±8	97±1	104±2	0.003	0.308	0.214
HR, bpm	585±23	581±30	574±11	597±8	0.291	0.758	0.396
Glomerular filtration rate (n=7 LF, n=11 HF)							
GFR, μ L/min per 100 g BW	1039±96	1053±51	960±46	778±25	0.249	0.019	0.067
Autonomic function, Δ from baseline (n=8–9 LF, n=10 HF)							
Δ MAP mecamylamine, mm Hg	-3.2±3.3	-7.4±2.0	-5.7±2.8	-17.2±1.3†	0.026	0.006	0.048
Δ HR propranolol, bpm	-42.9±11.1	-31.9±12.1	-37.5±15.2	-83.9±12.1	0.086	0.189	0.037
Δ MAP prazosin, mm Hg	-9.7±3.4	-7.3±3.7	-19.9±3.9	-36.0±3.2†	<0.0001	0.047	0.024
Δ HR atropine, bpm	-13.4±12.1	-21.8±13.7	-3.9±14.5	-3.5±20.5	0.912	0.274	0.649

Data were analyzed by 2-way ANOVA followed by Tukey multiple comparisons post hoc test. Data were reported as mean±SEM. eWAT, epididymal white adipose tissue; GFR, glomerular filtration rate; HF, high fat diet; HR, heart rate; LF, low fat diet; MAP, mean arterial pressure; and MSEW, maternal separation and early weaning.

* P <0.05 vs MSEW-LF.

† P <0.05 vs control.

while capsaicin infusion increased MAP levels similarly in both groups. In mice fed a HF, eWAT stimulation with vehicle did not modify MAP in either group; however, capsaicin infusions increased MAP responses in obese MSEW mice compared with controls. The MAP peaked after 5 minutes of infusion and lasted for 30 minutes (Figure 1B). As shown in Figure 1C, the area under the curve of the MAP, calculated as the pressor response in a 30-minute period, was further increased in HF-fed MSEW compared with controls. Figure S3 shows that subcutaneous WAT did not respond to capsaicin infusions in either group. Therefore, these data indicate that capsaicin-induced blood pressure in obese MSEW mice is fat depot specific.

Neuronal Activation in Response to Vehicle and Capsaicin eWAT Stimulation

In control and MSEW mice fed a LF, the AAR stimulation with vehicle and capsaicin did not change the number of Fos positive cells in the OVLT, posterior PVN, RVLM, and NTS (Table S4A). Figure 2A shows representative microphotographs of Fos expression in the OVLT, PVN, and RVLM of control and MSEW mice fed a HF. Overall, capsaicin infusions in eWAT significantly increased the number of Fos positive cells in OVLT, posterior PVN, and RVLM in obese MSEW mice compared with vehicle infusions and capsaicin infusion in controls, whereas neuronal activation in NTS was similar between groups (Figure 2B). In addition to the OVLT, the other circumventricular organs quantified, the subfornical organ (SFO), and the area postrema (AP) showed no significant differences between groups, diets, and AAR stimulation (Table S4B). Also, capsaicin infusion in eWAT induced a similar increase in the number of Fos positive cells in the lateral parabrachial LPBN) and neuroendocrine neurons in the PVN and supraoptic nucleus, brain areas involved in pain sensing and response (Table S4B). Representative microphotographs of Fos-FG expression in the middle and posterior part of the PVN demonstrating no colocalization between Fos and FG in the PVN are shown in Figure S3A and S3B. Figure S4C shows representative images of Fos immunohistochemistry in NTS. Figure S4D shows schematic diagrams of the analyzed nuclei in stereotaxic coordinates of coronal sections.

Effect of RDNX on Acute AAR Stimulation and Chronic Blood Pressure

Under anesthesia, obese male mice from both groups subjected to a prior RDNX showed a ≈ 15 -mmHg MAP reduction (Figure 3A). Vehicle infusion did not influence MAP in either group; however, capsaicin infusion in eWAT significantly increased MAP in SHAM-MSEW mice compared with the SHAM-control group. When capsaicin was infused in eWAT of mice that underwent RDNX,

the acute increase in MAP was blunted. In addition, RDNX lowered MAP in obese control and MSEW conscious mice (Figure 3B), abolishing the blood pressure differences between groups. Norepinephrine content in renal cortexes, as a general indication of the degree of innervation of these kidneys, was reduced in both acute and chronic experiments (Figure 3C). Noteworthy, the results we have obtained in the SHAM operated mice in response to capsaicin replicate the findings reported in a separate set of intact mice in Figure 1B.

Selective Sensory Denervation in eWAT

To further assess the contribution of the AAR in the exacerbated obesity-induced hypertension displayed by in MSEW, mice were subjected to selective afferent denervation using RTX. As shown in Figure 4A, bilateral eWAT infusions with vehicle did not change MAP from baseline in both groups. Sensory denervation significantly decreased MAP only in MSEW mice, a reduction that lasted for 3 days. Figure 4B shows the differences in 24-hour MAP after SHAM or RTX surgeries. In addition, the greater mecamylamine-induced decrease in blood pressure from baseline in MSEW-SHAM mice was blunted after RTX ablation (Figure 4C). Validation of the afferent-selective RTX denervation assessed by intravital 2-photon microscopy using the Calca reporter mouse is shown in Figure 4D. Focal denervation areas after 5 days can be observed in Figure S5.

RT-qPCR of Targets Linked to Sensory Stimulation in eWAT

Figure 5A shows the gene expression panel of factors and receptors that are known to increase/mediate the activity of sensory neurons. No significant gene expression changes in LF-fed control and MSEW mice were observed (Table S4). In HF-fed MSEW mice, mRNA expression of Tph1 was significantly increased compared with controls, while Htr2a mRNA expression was elevated but not statistically different (Figure 5A). Further, eWAT serotonin concentration was significantly higher in MSEW compared with controls (Figure 5B).

DISCUSSION

This study shows that afferent signals from eWAT contribute to exacerbating the sympathetic activation and hypertension in male HF-fed MSEW mice. The acute stimulation of eWAT with capsaicin induced a greater increase in the blood pressure response and increased the neuronal activation in the OVLT, PVN, and RVLM in obese MSEW mice, despite similar amount of adiposity and circulating leptin levels compared with obese

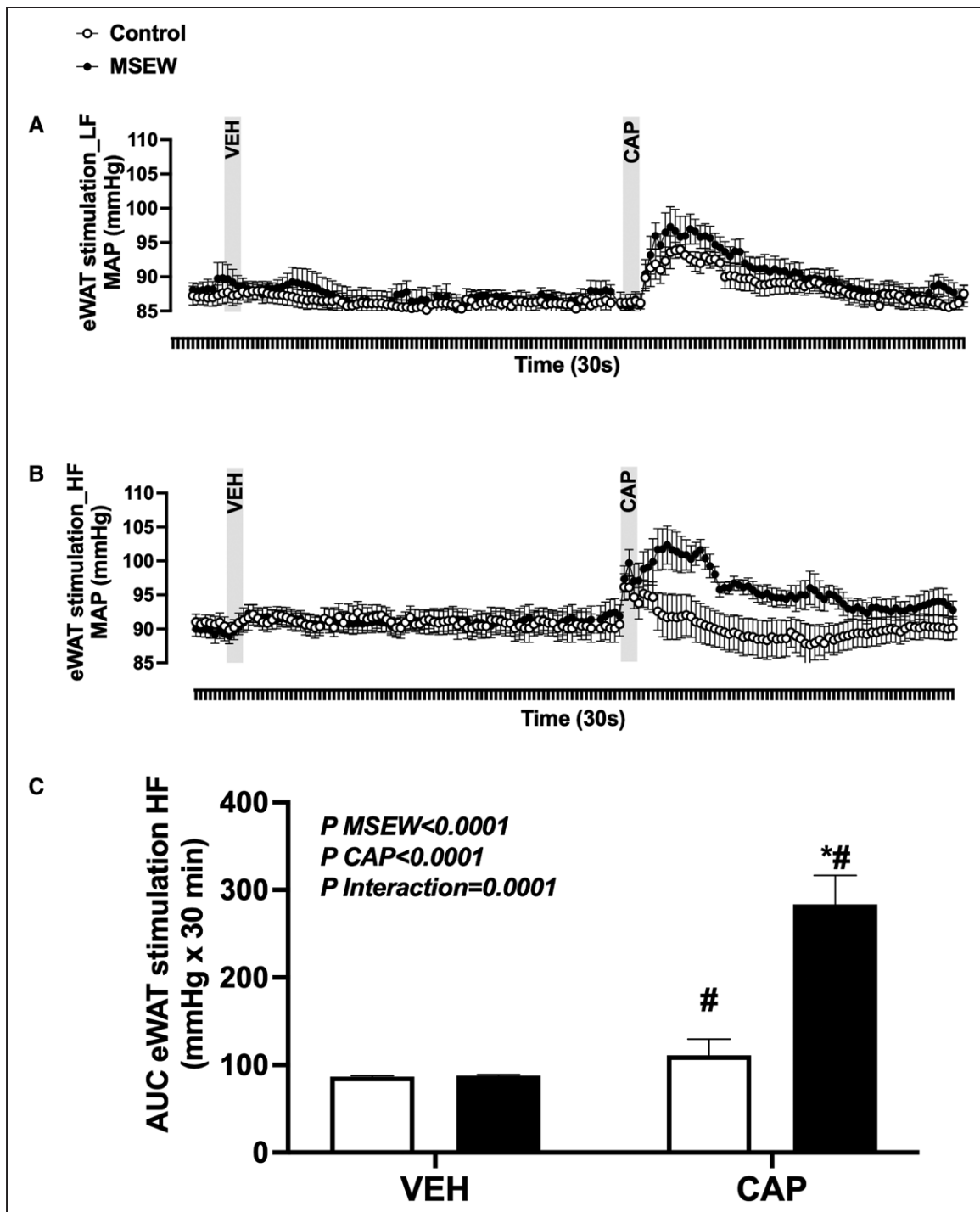


Figure 1. Acute eWAT stimulation with capsaicin (CAP) exacerbated mean arterial pressure (MAP) response in obese MSEW male mice.

A, Blood pressure trace in mice fed a low fat diet (LF). **B**, Blood pressure trace in mice fed a high fat diet (HF) **(C)**, 30-min area under the curve (AUC) in response to CAP. Data were analyzed by ANOVA repeated measures for continuous blood pressure trace and 2-way ANOVA followed by Tukey multiple comparisons post hoc test for AUC analysis. Data were reported as mean \pm SEM. n=8 per group. eWAT indicates epididymal white adipose tissue; MSEW, maternal separation and early weaning; and VEH, vehicle. * $P < 0.05$ vs control.

control mice. In addition, renal denervation prevented the chronic elevation of blood pressure and the acute capsaicin-induced pressor response in obese MSEW mice. Furthermore, selective afferent eWAT denervation reduced the blood pressure response and attenuated

the sympathetic index in these mice. Finally, we identified local serotonin as a potential endogenous factor that may stimulate the afferent sensory neurons. Taken together, these data indicate that male mice exposed to MSEW display exacerbated sympathetic

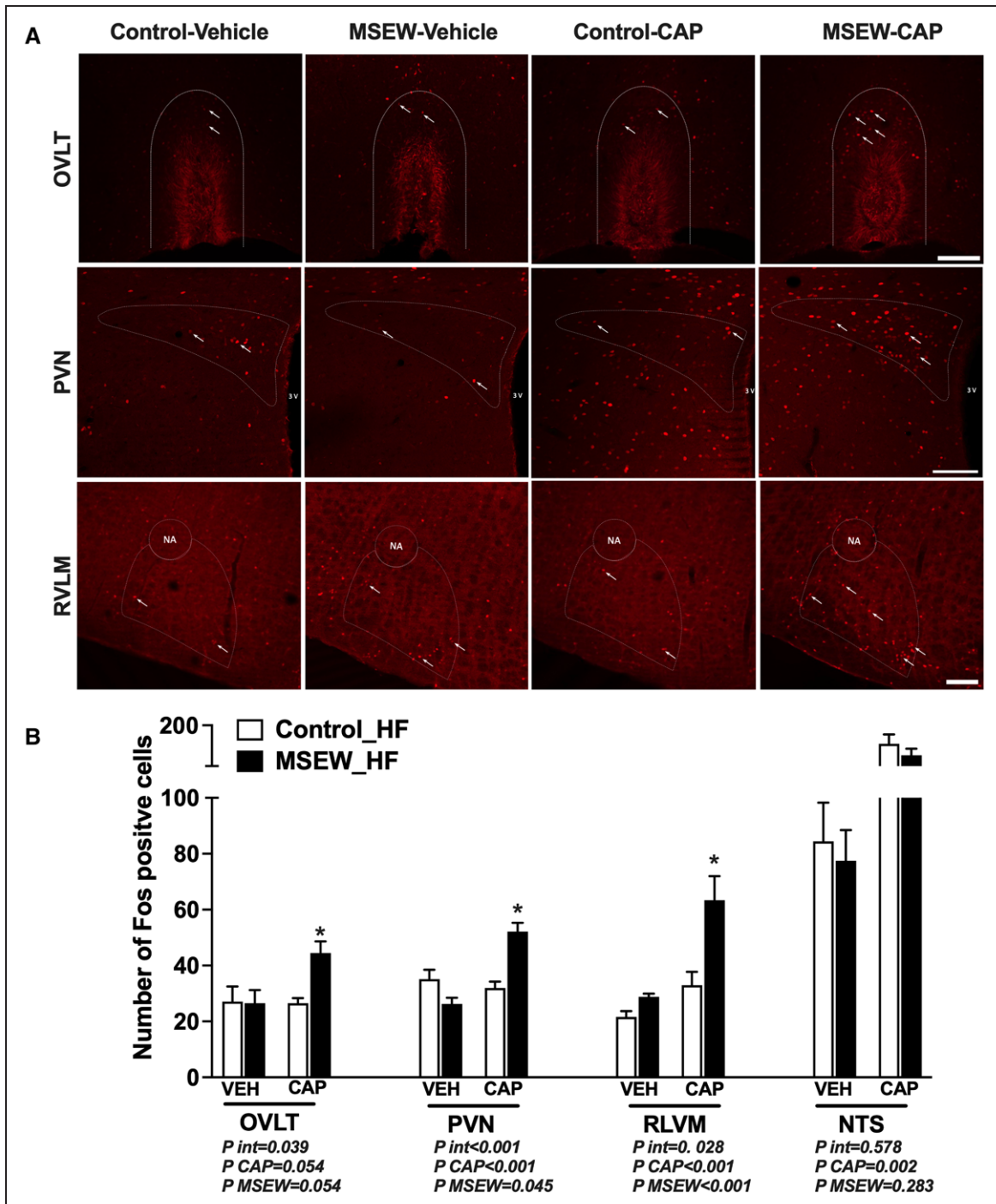


Figure 2. Acute eWAT stimulation with capsaicin (CAP) increases neuronal activation in organum vasculosum of the lamina terminalis (OVLT), paraventricular nucleus of the hypothalamus (PVN), and rostroventrolateral medulla (RVLM) in obese MSEW male mice.

A, Pattern of Fos immunoreactivity in the OVLT (0.50 mm from bregma; **top**), posterior PVN (−1.06 mm from bregma; **middle**), and RVLM (−6.72 mm from bregma; **bottom**) of control and MSEW mice infused with vehicle (VEH) or CAP in eWAT. A dotted shape delimits the brain areas in each image in which the quantification was performed.⁹⁵ White arrows indicate Fos positive cells. Microphotographs (×10) for OVLT, PVN, and RVLM were acquired using upright Zeiss LSM 880 multiphoton microscope and ZEISS ZEN Digital Imaging for Light Microscopy software (cFos: red filter). Scale bar, 100 μm. Representative schematic figures in stereotaxic coordinates for each brain area analyzed are included in the [Data Supplement](#). **B**, Average number of Fos positive cells in OVLT, posterior PVN, RVLM, and nucleus of the solitary tract (NTS) control and MSEW mice infused with VEH or CAP in eWAT. Data were analyzed by 2-way ANOVA followed by Tukey multiple comparisons post hoc test. Data were reported as mean±SEM. n=6-7 per group. For Fos positive cell quantification, ×10 magnification images were visualized with Nikon Super Resolution Inverted Microscope (cFos: red filter) and acquired with Nikon NIS-Elements (NIS-Elements Software, version 4.00.08; Nikon Instruments, Inc). 3 V indicates third ventricle; eWAT, epididymal white adipose tissue; MSEW, maternal separation early weaning; and NA, nucleus ambiguus. * $P<0.05$ vs MSEW-high fat (HF), VEH and control-HF CAP.

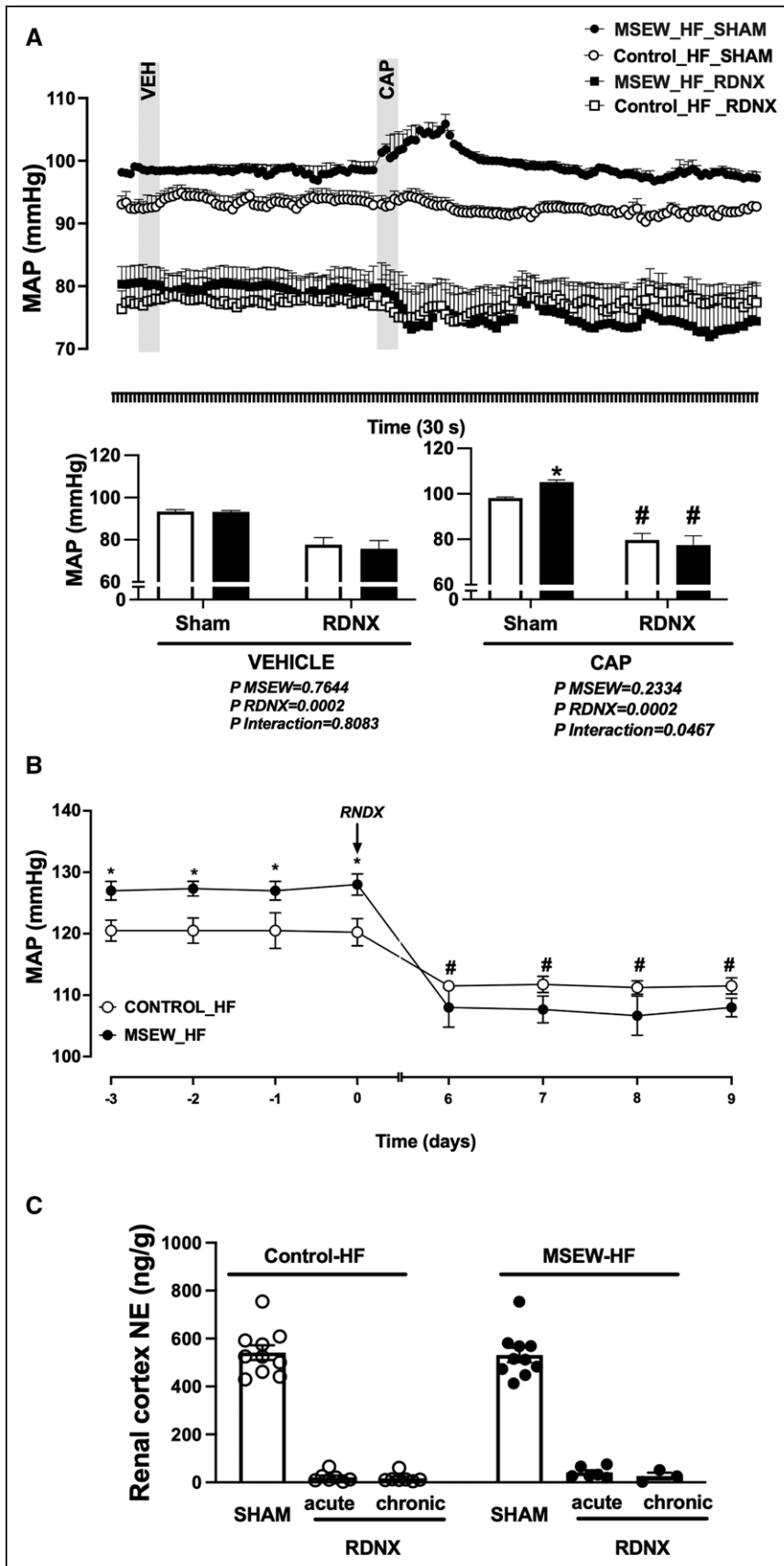


Figure 3. Renal denervation abolishes the differences in blood pressure in obese MSEW male mice. **A**, Bilateral renal denervation (RDNX) abolished the acute changes in mean arterial pressure (MAP) in response to epididymal white adipose tissue stimulation with capsaicin (CAP). **B**, RDNX blunts the differences in chronic MAP. **C**, Renal cortex norepinephrine (NE) content was dramatically reduced in all mice subjected to RDNX. Data were analyzed by 2-way ANOVA followed by Tukey multiple comparisons post hoc test. Data were reported as mean±SEM. n=5 to 6 per group. HF indicates high fat diet; MSEW, maternal separation early weaning; and VEH, vehicle. **P*<0.05 vs control; #*P*<0.05 vs SHAM.

outflow to the kidneys when fed a HF, eliciting long-term increased blood pressure. This heightened sympathetic outflow is most likely mediated, in part, by

afferent signals from eWAT projecting to brain nuclei with a pivotal role in the development of neurogenic hypertension.

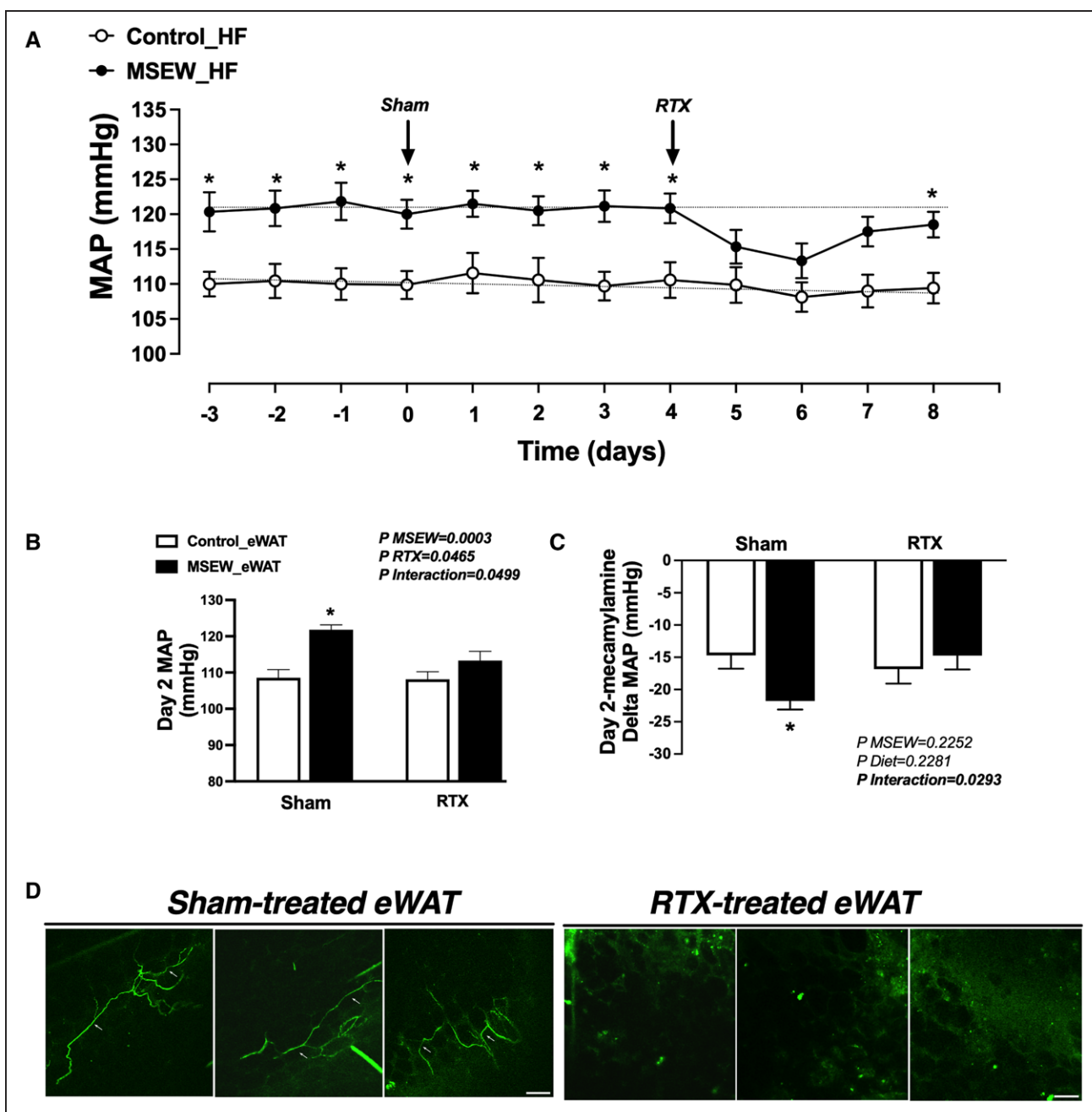


Figure 4. Selective afferent denervation in eWAT lowers blood pressure and sympathetic index in obese MSEW male mice.

A, Blood pressure trace before and after resiniferotoxin (RTX) injections in eWAT. **B**, Twenty-four-hour blood pressure after 2 d of sham or RTX surgery. **C**, Acute mecamylamine-induced blood pressure reduction. **D**, Representative images of Sham and RTX-treated eWAT using the CGRP (calcitonin gene-related peptide) reporter for sensory neuron Calca mouse. White arrows indicate the GFP (green fluorescence protein) labeled sensory neurons in eWAT. Intravital imaging of exposed fat pads was assessed on the stage of the multiphoton photon microscope (30 Hz full frame acquisition, Scientifica, Ltd, Uckfield, United Kingdom) using a 16X Nikon objective. Green pseudo coloring and contrast were applied after images were acquired using Image J processing software (Image J 1.53c, <http://imagej.nih.gov/ij/>; National Institutes of Health). Scale bar, 50 μ m. Data were analyzed by 2-way ANOVA followed by Tukey multiple comparisons post hoc test. Data were reported as mean \pm SEM. n=8 per group. HF indicates high fat diet; eWAT, epididymal white adipose tissue; MAP, mean arterial pressure; and MSEW, maternal separation early weaning. * P <0.05 vs control.

Compared with essential hypertension in lean subjects, obesity-related hypertension has an important neurogenic component and is characterized by sympathetic hyperactivity to the kidneys and skeletal muscle

vasculature and an absence of the suppression of the cardiac sympathetic outflow seen in the normotensive, obese subjects.^{39–41} Renal nerve ablation is a current approach to control drug-resistant hypertension in

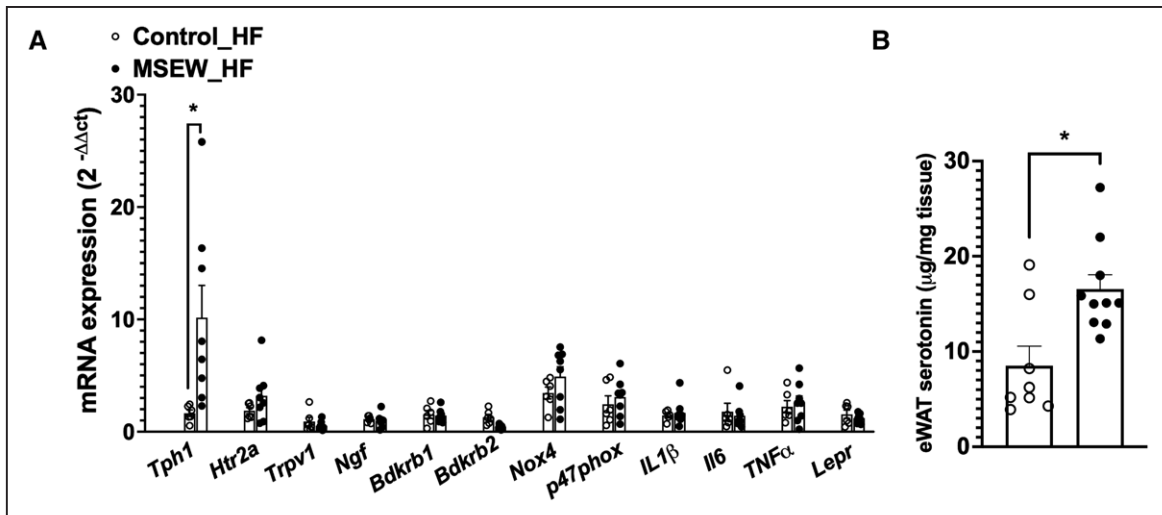


Figure 5. Obese MSEW male mice display increased serotonin content in epididymal eWAT.

A, RT-qPCR profiler showing significant increases in tryptophan hydroxylase 1. **B**, Serotonin content in eWAT determined by ELISA. Data were analyzed by the Student *t* test. Data were analyzed by 2-way ANOVA followed by Tukey multiple comparisons post hoc test when considering low fat (LF)–high fat (HF; Table SIV). Data were reported as mean±SEM. *n*=5 to 8 per group. Bdkrb1 indicates bradykinin receptor, beta 1; Bdkrb2, bradykinin receptor, beta 2; Htr2a, hydroxytryptamine (serotonin) receptor 2A; IL1β, interleukin 1 beta; IL6, interleukin-6; Lepr, leptin receptor; Ngf, nerve growth factor; NOX4, NADPH oxidase 4; p47phox (Ncf1), neutrophil cytosolic factor 1; Tnf, tumor necrosis factor; Tph1, tryptophan hydroxylase 1; and TrpV1, transient receptor potential cation channel, subfamily V, member 1. eWAT indicates epididymal white adipose tissue; MSEW, maternal separation early weaning; and RT-qPCR, Real Time quantitative Reverse Transcription Polymerase Chain Reaction. **P*<0.05 vs control.

humans, while numerous preclinical studies have shown its significant effect in different animal models of hypertension.^{42–46} Furthermore, the stimulation of renal afferent sensory neurons is implicated in renorenal reflexes that “enable total renal function to be self-regulated and balanced between the two kidneys” or a “self-regulated renorenal reflex loop.”^{47–49} It also has been proposed that the renal afferent reflex may play a critical role in chronic renal hypertension, especially when the baroreflex is impaired and activation of the renin-angiotensin system is reduced.⁵⁰

The presence of organ-specific sympathetic neural activation in human obesity is now accepted. The contribution of hyperinsulinemia, high plasma leptin levels, obstructive sleep apnea, and reduced gain of the arterial baroreflex has been widely studied as underlying mechanisms.^{10,51–54} In studies using a combination of trans-synaptic retrograde viral tract tracers with an anterograde transneuronal viral tract tracer into the inguinal WAT or eWAT of rats and Siberian hamsters, Bartness et al were able to demonstrate a cross talk between the central nervous system and the adipose tissue.^{15,17,55,56} In these studies, sensory neurons that innervate WAT project from the dorsal root ganglia to OVLT, PVN, RVLM, and NTS among other brain areas.^{17,57,58} The PVN is one of the major integrative centers in the brain that receives sensory signals from the periphery and regulates sympathetic nervous system outflow and cardiovascular function via the activation of preautonomic neurons that project to the RVLM, NTS, and spinal cord.^{59–63} In

addition, the, OVLT—a circumventricular organ that lacks a complete blood-brain barrier and is in direct contact with the plasma and cerebrospinal fluid—also projects to the PVN, contributing to blood pressure regulation.^{64–66}

Maternal separation is used as a rodent paradigm of early life stress.²¹ Several studies have shown that male rats subjected to maternal separation are normotensive when kept on a normal diet while displaying mild effects on cardiac autonomic balance and heart structure and reduced renal function.⁶⁷ Specifically, lower glomerular filtration rate was normalized after renal denervation, and the renal dysfunction was associated with the α-adrenergic receptor desensitization in isolated renal vasculature.^{34,68,69} Furthermore, borderline hypertensive rats exposed to maternal separation display enhanced neuronal activation and cardiovascular responses to acute stress.³² Male control and maternally separated rats fed a HF for 22 weeks display similar blood pressure and body weight.⁷⁰ However, in this study, we reported that male mice exposed to MSEW show sympathetic activation associated with increased blood pressure despite similar amount of adiposity and plasma leptin levels compared with control mice. Accordingly, the in vivo and in vitro assays using a β3-adrenergic receptor agonist indicate that sympathetic activation does not promote lipolysis to prevent fat expansion in obese MSEW male mice. Moreover, we demonstrated that bilateral renal denervation abolished the chronic blood pressure differences between control and MSEW mice. Renal denervation also abrogated the exacerbated

acute pressor response to capsaicin infused in eWAT seen in obese MSEW mice. Taken together, these data indicate that renal nerves play a critical role as the efferent arm of the AAR. This scenario points to a neurogenic mechanism implicated in the sensitization of the acute and chronic blood pressure response displayed by obese male MSEW mice.

Several studies have reported that maternal separation induces neuronal activation in PVN.^{30,32,71} However, these studies do not provide in depth neuronal characterization within the PVN. In the present study, using Fos expression as a marker of neuronal activation, we observed that eWAT stimulation with capsaicin increased the neuronal activation of nonendocrine neurons in the posterior PVN and RVLM in obese MSEW mice. Based on these results, we speculate that these activated neurons in the posterior PVN are most likely preautonomic and, project to RVLM, and therefore, are responsible for increasing blood pressure in response to capsaicin stimulation. However, further neuroanatomical and functional studies are needed to demonstrate that these neurons in the posterior PVN receive afferent signals from eWAT and project to the brain stem regulating sympathetic tone and blood pressure. Our results also showed increased capsaicin-induced neuronal activation in the OVLT of obese MSEW males. However, based on the approach utilized in this study, we cannot determine that these neurons receive afferent signals directly from eWAT or project to the PVN.

To further assess the contribution of depot-specific afferent signals on blood pressure responses, we ablated the sensory neurons with RTX—a TRPV1 agonist that functions as a 1000× more potent capsaicin analog and destroys sensory neurons.^{72–75} Bilateral denervation of eWAT with RTX reduced blood pressure in MSEW males fed HF to similar levels as control mice suggesting that fat afferent activity could be responsible for the increased blood pressure and sympathetic activity in MSEW mice. The measurement of afferent eWAT nerve activity and efferent renal nerve activity will provide irrefutable evidence of the sensitization of the fat–brain–blood pressure axis in obese MSEW mice.

One of the main findings of this study is that obese MSEW mice show greater blood pressure sensitivity to acute eWAT stimulation. Although capsaicin is not an endogenous ligand, it has been widely used to study its excitatory afferent effects and the physiological function of afferent neurons. Xiong et al¹¹ have shown that obese hypertensive rats display greater WAT afferent nerve activity and RSNA in response to capsaicin.¹⁸ Moreover, in previous studies, Nijima has reported similar nerve activity increases after stimulating adipose tissue depots with leptin.¹⁴ To investigate a possible endogenous factor that could chronically activate the sensory neurons in eWAT from MSEW mice, we analyzed a range of potential ligands and receptors expressed in

these neurons. Based on the literature, we tested the gene expression of several potential ligands stimulating the sensory neurons in eWAT, including oxidative stress, inflammation, prostaglandins, bradykinin, and different growth factors.^{76–80} Nevertheless, only Tph1 showed a significant upregulation in MSEW mice fed HF. Serotonin (5-HT) is synthesized by Tph1 (peripheral expression) and Tph2 (central nervous system expression). Inhibition of peripheral 5-HT synthesis (eg, telotristat) is a novel therapeutic strategy for pulmonary hypertension, inflammatory diseases, thrombosis, and obesity, aiming to avoid the adverse effects of Tph2 inhibition on the central nervous system.⁸¹ Tph1 enzyme is the rate-limiting step of serotonin biosynthesis by mastocytes,⁸² macrophages,⁸³ and adipocytes.^{84,85} Thus, we identified Tph1-derived serotonin as a potential endogenous stimulator of the sensory neurons in eWAT from MSEW mice. The mechanism by which MSEW upregulates Tph1 expression remains under investigation.

Serotonin can activate sensory neurons directly by binding to 5HT 2, 3, 4, and 7 receptors.^{86–89} In addition, it has been shown that this specific ligand-receptor interaction induces GPCR-mediated PKC (protein kinase C) to phosphorylate TRPV1 channels increasing the sensory neuron activation.^{90,91} Moreover, 5HT can indirectly sensitize sensory neurons by binding to 5-HT2 receptors and triggering PKC activation that increases the expression of neuronal acid-sensing ion channels in the neurons.^{92,93} These channels sense extracellular protons and mediate increased signaling during sensory stimulation such as pain.^{90,94}

In the current study, we found that a subset of TRPV1+ sensory afferents could be implicated in greater capsaicin-induced blood pressure increases in obese MSEW mice via the direct connection with PVN-RVLM, contributing to chronic AAR stimulation. We also stimulated pain-sensing neurons projecting to magnocellular neurons in the lateral magnocellular division of the PVN (PaML), supraoptic nucleus, and lateral parabrachial nucleus brain areas involved in pain-sensing and response^{95–97}; however, we found similar capsaicin-induced neuronal activation in both control and MSEW obese mice. Future studies will address whether this effect also extends to other populations of sensory neurons, such as low-threshold mechanoreceptors. These afferents could be further characterized, for instance, by performing anterograde and retrograde neuronal tracers in combination with electrophysiology or calcium imaging from dissociated dorsal root ganglia neurons in culture, which would allow us to determine whether increased local serotonin displayed by obese MSEW mice is responsible for the afferent neuron activation in eWAT. While exogenous capsaicin specifically stimulates TRPV1 channels, this study does not allow the conclusion of whether the excitability of the sensory neuron is exclusive to TRPV1 activation. Therefore, in addition

to the increased serotonin levels, AAR hypersensitivity could be given by increased terminal branching of sensory afferents, the plasticity of sensory neuron synapses onto spinal neurons, such as alteration in CGRP or substance P release, or an overall increase in the number of nociceptors in response to early life stress. As a result, increases in sensory neuron innervation and excitability in eWAT could be determined by quantifying the number and excitability of peptidergic/nonpeptidergic nociceptors in dorsal ganglia root cultures.

Of note, we have shown that both male and female MSEW mice display exacerbated hypertension associated with HF feeding; however, only females show greater adiposity and metabolic compromise compared with control mice.^{98,99} Thus, male MSEW mice show neurogenic hypertension, while female MSEW mice appear to develop hypertension secondary to cardiometabolic dysfunction. This is in accordance with other studies of developmental programming where similar mechanisms underlying sex differences have been described.¹⁰⁰ To consider other potential mechanisms underlying hypertension in our model, the greater acute responses to mecamylamine and prazosin in obese MSEW mice suggest an important contribution of the systemic vasculature and the control of total peripheral resistance. In addition, acute and long-term changes in blood pressure in our mice undergoing total renal denervation indicate a similar importance of the renal vasculature in our model. However, chronic inhibition of systemic vascular constriction may provide additional evidence of the contribution of other vascular beds as well.

In conclusion, this study shows that afferent sensory signals derived from eWAT may contribute to the exacerbated fat–brain–blood pressure axis in male mice exposed to early life stress. Also, we propose that increased local serotonin levels, or the hyperresponsiveness of sensory neurons itself, could contribute to the mechanism by which MSEW displays exacerbated neuronal activation in PVN and RVLM. Thus, AAR may further enhance the physiological cardiovascular response to HF, as male MSEW mice show higher blood pressure than controls while having similar increases in fat mass and circulating leptin. In addition, this increase in blood pressure is most likely neurogenic, as an α -receptor blocker or renal denervation induced significant changes in resting blood pressure. Nevertheless, extending this study to afferent signals from kidney and perirenal fat will provide a better understanding of the contribution of afferent signals during obesity-induced hypertension in this model.

PERSPECTIVES

Using a mouse model, this study shows that early life stress enhances the reactivity of the fat–brain–blood pressure axis during obesity. As obesity increases the

risk of drug-resistant hypertension, identifying novel underlying mechanisms may help developing therapeutic approaches for successfully managing neurogenic hypertension associated with obesity, particularly in patients affected by nontraditional risk factors. A comprehensive understanding of how afferent reflexes could exacerbate blood pressure in subjects exposed to adverse childhood experiences (ACEs) or any other kind of early life insults could provide insights to improve personalized antihypertensive therapeutic approaches.

ARTICLE INFORMATION

Received March 22, 2021; accepted August 19, 2021.

Affiliations

Department of Pharmacology and Nutritional Sciences, College of Medicine (C.D., J.R.L., S.G., N.A., O.T., A.S.L.) and Department of Biology, College of Arts and Sciences (E.R.S., J.L.O.), University of Kentucky, Lexington.

Acknowledgments

We thank Dr Kimberly Nixon for sharing her expertise in brain immunohistochemistry, and Dr Ruei-Lung Lin for the acquisition of intravital microscopy images at the Sanders-Brown Intravital Imaging Facility at University of Kentucky, and Dr Sean Stocker for his valuable feedback on this project. We also thank Thomas Dolan for his assistance in developing the graphical abstract. We would like to acknowledge the imaging service from Thomas Wilkop from the Light Microscopy Core at University of Buenos Aires.

Sources of Funding

This study was supported by grants from the NIH National Heart, Lung, and Blood Institute (R01 135158 to ASL), the Kentucky Center of Research in Obesity and Cardiovascular Disease COBRE (P20 GM103527), Light Microscopy Core at the University of Kentucky is, in part, supported by the Office of the Vice President for Research.

Disclosures

None.

Supplemental Materials

Expanded Materials and Methods
Data Supplement Tables S1–S4
Data Supplement Figures S1–S5

REFERENCES

- Hales CM, Fryar CD, Carroll MD, Freedman DS, Ogden CL. Trends in obesity and severe obesity prevalence in US youth and adults by sex and age, 2007–2008 to 2015–2016. *JAMA*. 2018;319:1723–1725. doi: 10.1001/jama.2018.3060
- Centers for Disease Control and Prevention. Overweight and Obesity. Data & Statistics, updated June 7, 2021. <https://www.cdc.gov/obesity/data/adult.html>
- Hall JE, do Carmo JM, da Silva AA, Wang Z, Hall ME. Obesity-induced hypertension: interaction of neurohumoral and renal mechanisms. *Circ Res*. 2015;116:991–1006. doi: 10.1161/CIRCRESAHA.116.305697
- Lohmeier TE, Iliescu R. The sympathetic nervous system in obesity hypertension. *Curr Hypertens Rep*. 2013;15:409–416. doi: 10.1007/s11906-013-0356-1
- Lambert EA, Esler MD, Schlaich MP, Dixon J, Eikelis N, Lambert GW. Obesity-associated organ damage and sympathetic nervous activity. *Hypertension*. 2019;73:1150–1159. doi: 10.1161/HYPERTENSIONAHA.118.11676
- Hirooka Y. Sympathetic activation in hypertension: importance of the central nervous system. *Am J Hypertens*. 2020;33:914–926. doi: 10.1093/ajh/hpaa074
- Kalil GZ, Haynes WG. Sympathetic nervous system in obesity-related hypertension: mechanisms and clinical implications. *Hypertens Res*. 2012;35:4–16. doi: 10.1038/hr.2011.173

8. Simonds SE, Cowley MA. Hypertension in obesity: is leptin the culprit? *Trends Neurosci.* 2013;36:121–132. doi: 10.1016/j.tins.2013.01.004
9. Caron A, Lee S, Elmquist JK, Gautron L. Leptin and brain–adipose cross-talks. *Nat Rev Neurosci.* 2018;19:153–165. doi: 10.1038/nrn.2018.7
10. Shi Z, Pelletier NE, Wong J, Li B, Sdrulla AD, Madden CJ, Marks DL, Brooks VL. Leptin increases sympathetic nerve activity via induction of its own receptor in the paraventricular nucleus. *Elife.* 2020;9:e55357. doi: 10.7554/eLife.55357
11. Xiong XQ, Chen WW, Han Y, Zhou YB, Zhang F, Gao XY, Zhu GQ. Enhanced adipose afferent reflex contributes to sympathetic activation in diet-induced obesity hypertension. *Hypertension.* 2012;60:1280–1286. doi: 10.1161/HYPERTENSIONAHA.112.198002
12. Xiong XQ, Chen WW, Zhu GQ. Adipose afferent reflex: sympathetic activation and obesity hypertension. *Acta Physiol (Oxf).* 2014;210:468–478. doi: 10.1111/apha.12182
13. Cao W, Shi M, Wu L, Li J, Yang Z, Liu Y, Wilcox CS, Hou FF. Adipocytes initiate an adipose-cerebral-peripheral sympathetic reflex to induce insulin resistance during high-fat feeding. *Clin Sci (Lond).* 2019;133:1883–1899. doi: 10.1042/CS20190412
14. Nijima A. Afferent signals from leptin sensors in the white adipose tissue of the epididymis, and their reflex effect in the rat. *J Auton Nerv Syst.* 1998;73:19–25. doi: 10.1016/s0165-1838(98)00109-x
15. Bowers RR, Festuccia WT, Song CK, Shi H, Migliorini RH, Bartness TJ. Sympathetic innervation of white adipose tissue and its regulation of fat cell number. *Am J Physiol Regul Integr Comp Physiol.* 2004;286:R1167–R1175. doi: 10.1152/ajpregu.00558.2003
16. Bartness TJ, Liu Y, Shrestha YB, Ryu V. Neural innervation of white adipose tissue and the control of lipolysis. *Front Neuroendocrinol.* 2014;35:473–493. doi: 10.1016/j.yfrne.2014.04.001
17. Ryu V, Bartness TJ. Short and long sympathetic-sensory feedback loops in white fat. *Am J Physiol Regul Integr Comp Physiol.* 2014;306:R886–R900. doi: 10.1152/ajpregu.00060.2014
18. Shi Z, Chen WW, Xiong XQ, Han Y, Zhou YB, Zhang F, Gao XY, Zhu GQ. Sympathetic activation by chemical stimulation of white adipose tissues in rats. *J Appl Physiol (1985).* 2012;112:1008–1014. doi: 10.1152/jappphysiol.01164.2011
19. Shi Z, Wang YF, Wang GH, Wu YL, Ma CL. Paraventricular nucleus is involved in the central pathway of adipose afferent reflex in rats. *Can J Physiol Pharmacol.* 2016;94:534–541. doi: 10.1139/cjpp-2015-0097
20. Dalmasso C, Leachman JR, Osborn JL, Loria AS. Sensory signals mediating high blood pressure via sympathetic activation: role of adipose afferent reflex. *Am J Physiol Regul Integr Comp Physiol.* 2020;318:R379–R389. doi: 10.1152/ajpregu.00079.2019
21. Murphy MO, Cohn DM, Loria AS. Developmental origins of cardiovascular disease: impact of early life stress in humans and rodents. *Neurosci Biobehav Rev.* 2017;74(Pt B):453–465. doi: 10.1016/j.neubiorev.2016.07.018
22. Hao G, Wang X, Treiber FA, Harshfield G, Kapuku G, Su S. Body mass index trajectories in childhood is predictive of cardiovascular risk: results from the 23-year longitudinal Georgia Stress and Heart study. *Int J Obes (Lond).* 2018;42:923–925. doi: 10.1038/ijo.2017.244
23. Su S, Wang X, Kapuku GK, Treiber FA, Pollock DM, Harshfield GA, McCall WV, Pollock JS. Adverse childhood experiences are associated with detrimental hemodynamics and elevated circulating endothelin-1 in adolescents and young adults. *Hypertension.* 2014;64:201–207. doi: 10.1161/HYPERTENSIONAHA.113.02755
24. Su S, Wang X, Pollock JS, Treiber FA, Xu X, Snieder H, McCall WV, Stefanek M, Harshfield GA. Adverse childhood experiences and blood pressure trajectories from childhood to young adulthood: the Georgia stress and Heart study. *Circulation.* 2015;131:1674–1681. doi: 10.1161/CIRCULATIONAHA.114.013104
25. Wiss DA, Brewerton TD. Adverse childhood experiences and adult obesity: a systematic review of plausible mechanisms and meta-analysis of cross-sectional studies. *Physiol Behav.* 2020;223:112964. doi: 10.1016/j.physbeh.2020.112964
26. Carlyle BC, Duque A, Kitchen RR, Bordner KA, Coman D, Doolittle E, Papademetris X, Hyder F, Taylor JR, Simen AA. Maternal separation with early weaning: a rodent model providing novel insights into neglect associated developmental deficits. *Dev Psychopathol.* 2012;24:1401–1416. doi: 10.1017/S095457941200079X
27. George ED, Bordner KA, Elwafi HM, Simen AA. Maternal separation with early weaning: a novel mouse model of early life neglect. *BMC Neurosci.* 2010;11:123. doi: 10.1186/1471-2202-11-123
28. Murphy MO, Herald JB, Leachman JR, Villasante Tezanos A, Cohn DM, Loria AS. A model of neglect during postnatal life heightens obesity-induced hypertension and is linked to a greater metabolic compromise in female mice. *Int J Obes (Lond).* 2018;42:1354–1365. doi: 10.1038/s41366-018-0035-z
29. Baracz SJ, Everett NA, Robinson KJ, Campbell GR, Cornish JL. Maternal separation changes maternal care, anxiety-like behaviour and expression of paraventricular oxytocin and corticotrophin-releasing factor immunoreactivity in lactating rats. *J Neuroendocrinol.* 2020;32:e12861. doi: 10.1111/jne.12861
30. Horii-Hayashi N, Sasagawa T, Matsunaga W, Matsue Y, Azuma C, Nishi M. Developmental changes in desensitisation of c-Fos expression induced by repeated maternal separation in pre-weaned mice. *J Neuroendocrinol.* 2013;25:158–167. doi: 10.1111/j.1365-2826.2012.02377.x
31. Nishi M, Horii-Hayashi N, Sasagawa T. Effects of early life adverse experiences on the brain: implications from maternal separation models in rodents. *Front Neurosci.* 2014;8:166. doi: 10.3389/fnins.2014.00166
32. Sanders BJ, Anticevic A. Maternal separation enhances neuronal activation and cardiovascular responses to acute stress in borderline hypertensive rats. *Behav Brain Res.* 2007;183:25–30. doi: 10.1016/j.bbr.2007.05.020
33. Dalmasso C, Chade AR, Mendez M, Giani JF, Bix GJ, Chen KC, Loria AS. Intrarenal renin angiotensin system imbalance during post-natal life is associated with increased microvascular density in the mature kidney. *Front Physiol.* 2020;11:1046. doi: 10.3389/fphys.2020.01046
34. Loria AS, Brands MW, Pollock DM, Pollock JS. Early life stress sensitizes the renal and systemic sympathetic system in rats. *Am J Physiol Renal Physiol.* 2013;305:F390–F395. doi: 10.1152/ajprenal.00008.2013
35. D'Angelo G, Loria AS, Pollock DM, Pollock JS. Endothelin activation of reactive oxygen species mediates stress-induced pressor response in Dahl salt-sensitive prehypertensive rats. *Hypertension.* 2010;56:282–289. doi: 10.1161/HYPERTENSIONAHA.110.152629
36. Schofield BR. Retrograde axonal tracing with fluorescent markers. *Curr Protoc Neurosci.* 2008;Chapter 1:Unit 1.17. doi: 10.1002/0471142301.n0117s43
37. McCoy ES, Taylor-Blake B, Zylka MJ. CGRP α -expressing sensory neurons respond to stimuli that evoke sensations of pain and itch. *PLoS One.* 2012;7:e36355. doi: 10.1371/journal.pone.0036355
38. McCoy ES, Taylor-Blake B, Street SE, Pribisko AL, Zheng J, Zylka MJ. Peptidergic CGRP α primary sensory neurons encode heat and itch and tonically suppress sensitivity to cold. *Neuron.* 2013;78:138–151. doi: 10.1016/j.neuron.2013.01.030
39. Esler M, Straznicki N, Eikelis N, Masuo K, Lambert G, Lambert E. Mechanisms of sympathetic activation in obesity-related hypertension. *Hypertension.* 2006;48:787–796. doi: 10.1161/01.HYP.0000242642.42177.49
40. Malpas SC. Sympathetic nervous system overactivity and its role in the development of cardiovascular disease. *Physiol Rev.* 2010;90:513–557. doi: 10.1152/physrev.00007.2009
41. Hugggett RJ, Burns J, Mackintosh AF, Mary DA. Sympathetic neural activation in nondiabetic metabolic syndrome and its further augmentation by hypertension. *Hypertension.* 2004;44:847–852. doi: 10.1161/01.HYP.0000147893.08533.d8
42. Gulati V, White WB. Novel approaches for the treatment of the patient with resistant hypertension: renal nerve ablation. *Curr Cardiovasc Risk Rep.* 2013;7:10.1007/s12170-12013-10334-12179. doi: 10.1007/s12170-013-0334-9
43. Osborn JW, Banek CT. Catheter-based renal nerve ablation as a novel hypertension therapy: lost, and then found, in translation. *Hypertension.* 2018;71:383–388. doi: 10.1161/HYPERTENSIONAHA.117.08928
44. Tzafiriri AR, Mahfoud F, Keating JH, Spognardi AM, Markham PM, Wong G, Highsmith D, O'Fallon P, Fuimaono K, Edelman ER. Procedural and anatomical determinants of multielectrode renal denervation efficacy. *Hypertension.* 2019;74:546–554. doi: 10.1161/HYPERTENSIONAHA.119.12918
45. Lerman LO, Kurtz TW, Touyz RM, Ellison DH, Chade AR, Crowley SD, Mattson DL, Mullins JJ, Osborn J, Eirin A, et al. Animal models of hypertension: a scientific statement from the american heart association. *Hypertension.* 2019;73:e87–e120. doi: 10.1161/HYP000000000000090
46. Foss JD, Wainford RD, Engeland WC, Fink GD, Osborn JW. A novel method of selective ablation of afferent renal nerves by periaxonal application of capsaicin. *Am J Physiol Regul Integr Comp Physiol.* 2015;308:R112–R122. doi: 10.1152/ajpregu.00427.2014
47. Kopp UC. Role of renal sensory nerves in physiological and pathophysiological conditions. *Am J Physiol Regul Integr Comp Physiol.* 2015;308:R79–R95. doi: 10.1152/ajpregu.00351.2014

48. Osborn JW, Tyshynsky R, Vulchanova L. Function of renal nerves in kidney physiology and pathophysiology. *Annu Rev Physiol*. 2021;83:429–450. doi: 10.1146/annurev-physiol-031620-091656
49. DiBona GF, Kopp UC. Neural control of renal function. *Physiol Rev*. 1997;77:75–197. doi: 10.1152/physrev.1997.77.1.75
50. Faber JE, Brody MJ. Afferent renal nerve-dependent hypertension following acute renal artery stenosis in the conscious rat. *Circ Res*. 1985;57:676–688. doi: 10.1161/01.res.57.5.676
51. da Silva AA, do Carmo JM, Li X, Wang Z, Mouton AJ, Hall JE. Role of hyperinsulinemia and insulin resistance in hypertension: metabolic syndrome revisited. *Can J Cardiol*. 2020;36:671–682. doi: 10.1016/j.cjca.2020.02.066
52. Shi Z, Zhao D, Cassaglia PA, Brooks VL. Sites and sources of sympathoexcitation in obese male rats: role of brain insulin. *Am J Physiol Regul Integr Comp Physiol*. 2020;318:R634–R648. doi: 10.1152/ajpregu.00317.2019
53. Venkataraman S, Vungarala S, Covassin N, Somers VK. Sleep apnea, hypertension and the sympathetic nervous system in the adult population. *J Clin Med*. 2020;9:591. doi: 10.3390/jcm9020591
54. Thorp AA, Schlaich MP. Relevance of sympathetic nervous system activation in obesity and metabolic syndrome. *J Diabetes Res*. 2015;2015:341583. doi: 10.1155/2015/341583
55. Nguyen NL, Randall J, Banfield BW, Bartness TJ. Central sympathetic innervations to visceral and subcutaneous white adipose tissue. *Am J Physiol Regul Integr Comp Physiol*. 2014;306:R375–R386. doi: 10.1152/ajpregu.00552.2013
56. Bartness TJ, Song CK. Brain-adipose tissue neural crosstalk. *Physiol Behav*. 2007;91:343–351. doi: 10.1016/j.physbeh.2007.04.002
57. Song CK, Schwartz GJ, Bartness TJ. Anterograde transneuronal viral tract tracing reveals central sensory circuits from white adipose tissue. *Am J Physiol Regul Integr Comp Physiol*. 2009;296:R501–R511. doi: 10.1152/ajpregu.90786.2008
58. Ryu V, Watts AG, Xue B, Bartness TJ. Bidirectional crosstalk between the sensory and sympathetic motor systems innervating brown and white adipose tissue in male Siberian hamsters. *Am J Physiol Regul Integr Comp Physiol*. 2017;312:R324–R337. doi: 10.1152/ajpregu.00456.2015
59. Guyenet PG, Stornetta RL, Holloway BB, Souza GMP, Abbott SGB. Rostral ventrolateral medulla and hypertension. *Hypertension*. 2018;72:559–566. doi: 10.1161/HYPERTENSIONAHA.118.10921
60. Sladek CD, Michelini LC, Stachenfeld NS, Stern JE, Urban JH. Endocrine-autonomic linkages. *Compr Physiol*. 2015;5:1281–1323. doi: 10.1002/cphy.c140028
61. Pyner S, Coote JH. Rostrolateral medulla neurons preferentially project to target-specified sympathetic preganglionic neurons. *Neuroscience*. 1998;83:617–631. doi: 10.1016/s0306-4522(97)00355-2
62. Becker BK. Shining light on the paraventricular nucleus: the role of glutamatergic PVN neurons in blood pressure control. *J Physiol*. 2018;596:6127–6128. doi: 10.1113/JP277043
63. Basting T, Xu J, Mukerjee S, Epling J, Fuchs R, Sriramula S, Lazartigues E. Glutamatergic neurons of the paraventricular nucleus are critical contributors to the development of neurogenic hypertension. *J Physiol*. 2018;596:6235–6248. doi: 10.1113/JP276229
64. Gabor A, Leenen FH. Central neuromodulatory pathways regulating sympathetic activity in hypertension. *J Appl Physiol (1985)*. 2012;113:1294–1303. doi: 10.1152/japplphysiol.00553.2012
65. Coote JH. A role for the paraventricular nucleus of the hypothalamus in the autonomic control of heart and kidney. *Exp Physiol*. 2005;90:169–173. doi: 10.1113/expphysiol.2004.029041
66. Shi P, Martinez MA, Calderon AS, Chen Q, Cunningham JT, Toney GM. Intra-carotid hyperosmotic stimulation increases Fos staining in forebrain organum vasculosum laminae terminalis neurons that project to the hypothalamic paraventricular nucleus. *J Physiol*. 2008;586:5231–5245. doi: 10.1113/jphysiol.2008.159665
67. Trombini M, Hulshof HJ, Graiani G, Carnevali L, Meerlo P, Quaini F, Sgoifo A. Early maternal separation has mild effects on cardiac autonomic balance and heart structure in adult male rats. *Stress*. 2012;15:457–470. doi: 10.3109/10253890.2011.639414
68. Loria AS, Yamamoto T, Pollock DM, Pollock JS. Early life stress induces renal dysfunction in adult male rats but not female rats. *Am J Physiol Regul Integr Comp Physiol*. 2013;304:R121–R129. doi: 10.1152/ajpregu.00364.2012
69. Loria AS, Osborn JL. Maternal separation diminishes α -adrenergic receptor density and function in renal vasculature from male Wistar-Kyoto rats. *Am J Physiol Renal Physiol*. 2017;313:F47–F54. doi: 10.1152/ajprenal.00591.2016
70. Loria AS, Spradley FT, Obi IE, Becker BK, De Miguel C, Speed JS, Pollock DM, Pollock JS. Maternal separation enhances anticontractile perivascular adipose tissue function in male rats on a high-fat diet. *Am J Physiol Regul Integr Comp Physiol*. 2018;315:R1085–R1095. doi: 10.1152/ajpregu.00197.2018
71. Sood A, Pati S, Bhattacharya A, Chaudhari K, Vaidya VA. Early emergence of altered 5-HT_{2A} receptor-evoked behavior, neural activation and gene expression following maternal separation. *Int J Dev Neurosci*. 2018;65:21–28. doi: 10.1016/j.ijdevneu.2017.10.005
72. Brown DC. Resiniferatoxin: the evolution of the “Molecular Scalpel” for chronic pain relief. *Pharmaceuticals (Basel)*. 2016;9:E47. doi: 10.3390/ph9030047
73. Szallasi A, Blumberg PM. Resiniferatoxin, a phorbol-related diterpene, acts as an ultrapotent analog of capsaicin, the irritant constituent in red pepper. *Neuroscience*. 1989;30:515–520. doi: 10.1016/0306-4522(89)90269-8
74. Szallasi A, Blumberg PM. Specific binding of resiniferatoxin, an ultrapotent capsaicin analog, by dorsal root ganglion membranes. *Brain Res*. 1990;524:106–111. doi: 10.1016/0006-8993(90)90498-z
75. Szolcsanyi J, Szallasi A, Szallasi Z, Joo F, Blumberg PM. Resiniferatoxin: an ultrapotent selective modulator of capsaicin-sensitive primary afferent neurons. *J Pharmacol Exp Ther*. 1990;255:923–928.
76. Pinho-Ribeiro FA, Verri WA Jr, Chiu IM. Nociceptor sensory neuron-immune interactions in pain and inflammation. *Trends Immunol*. 2017;38:5–19. doi: 10.1016/j.it.2016.10.001
77. Ma W, Quirion R. Inflammatory mediators modulating the transient receptor potential vanilloid 1 receptor: therapeutic targets to treat inflammatory and neuropathic pain. *Expert Opin Ther Targets*. 2007;11:307–320. doi: 10.1517/14728222.11.3.307
78. Gouin O, L’Herondelle K, Lebonvallet N, Le Gall-Ianotto C, Sakka M, Buhé V, Pléé-Gautier E, Carré JL, Lefeuvre L, Misery L, et al. TRPV1 and TRPA1 in cutaneous neurogenic and chronic inflammation: pro-inflammatory response induced by their activation and their sensitization. *Protein Cell*. 2017;8:644–661. doi: 10.1007/s13238-017-0395-5
79. Guilherme A, Henriques F, Bedard AH, Czech MP. Molecular pathways linking adipose innervation to insulin action in obesity and diabetes mellitus. *Nat Rev Endocrinol*. 2019;15:207–225. doi: 10.1038/s41574-019-0165-y
80. Dux M, Rosta J, Messlinger K. TRP channels in the focus of trigeminal nociceptor sensitization contributing to primary headaches. *Int J Mol Sci*. 2020;21:E342. doi: 10.3390/ijms21010342
81. Matthes S, Stadler J, Barton J, Leuschner G, Munker D, Arnold P, Villena-Hermoza H, Frankenberger M, Probst P, Koch A, et al. Asthma features in severe COPD: identifying treatable traits. *Respir Med*. 2018;145:89–94. doi: 10.1016/j.rmed.2018.10.027
82. Yabut JM, Desjardins EM, Chan EJ, Day EA, Leroux JM, Wang B, Crane ED, Wong W, Morrison KM, Crane JD, et al. Genetic deletion of mast cell serotonin synthesis prevents the development of obesity and insulin resistance. *Nat Commun*. 2020;11:463. doi: 10.1038/s41467-019-14080-7
83. Yabut JM, Crane JD, Green AE, Keating DJ, Khan WI, Steinberg GR. Emerging roles for serotonin in regulating metabolism: new implications for an ancient molecule. *Endocr Rev*. 2019;40:1092–1107. doi: 10.1210/er.2018-00283
84. Crane JD, Palanivel R, Mottillo EP, Bujak AL, Wang H, Ford RJ, Collins A, Blümer RM, Fullerton MD, Yabut JM, et al. Inhibiting peripheral serotonin synthesis reduces obesity and metabolic dysfunction by promoting brown adipose tissue thermogenesis. *Nat Med*. 2015;21:166–172. doi: 10.1038/nm.3766
85. Stunes AK, Reseland JE, Hauso O, Kidd M, Tømmerås K, Waldum HL, Syversen U, Gustafsson BI. Adipocytes express a functional system for serotonin synthesis, reuptake and receptor activation. *Diabetes Obes Metab*. 2011;13:551–558. doi: 10.1111/j.1463-1326.2011.01378.x
86. Salzer I, Gantumur E, Yousuf A, Boehm S. Control of sensory neuron excitability by serotonin involves 5HT_{2C} receptors and Ca²⁺-activated chloride channels. *Neuropharmacology*. 2016;110(pt A):277–286. doi: 10.1016/j.neuropharm.2016.08.006
87. Viguier F, Michot B, Hamon M, Bourgoin S. Multiple roles of serotonin in pain control mechanisms—implications of 5-HT₇ and other 5-HT receptor types. *Eur J Pharmacol*. 2013;716:8–16. doi: 10.1016/j.ejphar.2013.01.074
88. Loyd DR, Weiss G, Henry MA, Hargreaves KM. Serotonin increases the functional activity of capsaicin-sensitive rat trigeminal nociceptors via peripheral serotonin receptors. *Pain*. 2011;152:2267–2276. doi: 10.1016/j.pain.2011.06.002
89. Ohta T, Ikemi Y, Murakami M, Imagawa T, Otsuguro K, Ito S. Potentiation of transient receptor potential V1 functions by the activation of metabotropic 5-HT receptors in rat primary sensory neurons. *J Physiol*. 2006;576(pt 3):809–822. doi: 10.1113/jphysiol.2006.112250

90. Loyd DR, Henry MA, Hargreaves KM. Serotonergic neuromodulation of peripheral nociceptors. *Semin Cell Dev Biol*. 2013;24:51–57. doi: 10.1016/j.semcdb.2012.09.002
91. Vay L, Gu C, McNaughton PA. The thermo-TRP ion channel family: properties and therapeutic implications. *Br J Pharmacol*. 2012;165:787–801. doi: 10.1111/j.1476-5381.2011.01601.x
92. Qiu F, Qiu CY, Liu YQ, Wu D, Li JD, Hu WP. Potentiation of acid-sensing ion channel activity by the activation of 5-HT₂ receptors in rat dorsal root ganglion neurons. *Neuropharmacology*. 2012;63:494–500. doi: 10.1016/j.neuropharm.2012.04.034
93. Kweon HJ, Suh BC. Acid-sensing ion channels (ASICs): therapeutic targets for neurological diseases and their regulation. *BMB Rep*. 2013;46:295–304. doi: 10.5483/bmbrep.2013.46.6.121
94. White JP, Cibelli M, Rei Fidalgo A, Paule CC, Noormohamed F, Urban L, Maze M, Nagy I. Role of transient receptor potential and acid-sensing ion channels in peripheral inflammatory pain. *Anesthesiology*. 2010;112:729–741. doi: 10.1097/ALN.0b013e3181ca3179
95. Chiang MC, Bowen A, Schier LA, Tupone D, Uddin O, Heinricher MM. Parabrachial complex: a hub for pain and aversion. *J Neurosci*. 2019;39:8225–8230. doi: 10.1523/JNEUROSCI.1162-19.2019
96. Eliava M, Melchior M, Knobloch-Bollmann HS, Wahis J, da Silva Gouveia M, Tang Y, Ciobanu AC, Triana Del Rio R, Roth LC, Althammer F, et al. A new population of parvocellular oxytocin neurons controlling magnocellular neuron activity and inflammatory pain processing. *Neuron*. 2016;89:1291–1304. doi: 10.1016/j.neuron.2016.01.041
97. Bernard JF. Hypothalamus and nociceptive pathways. In: Schmidt RF, Willis WD, eds. *Encyclopedia of Pain*. Springer Berlin Heidelberg; 2007:944–948.
98. Dalmasso C, Leachman JR, Ensor CM, Yiannikouris FB, Giani JF, Cassis LA, Loria AS. Female mice exposed to postnatal neglect display angiotensin II-dependent obesity-induced hypertension. *J Am Heart Assoc*. 2019;8:e012309. doi: 10.1161/JAHA.119.012309
99. Leachman JR, Rea MD, Cohn DM, Xu X, Fondufe-Mittendorf YN, Loria AS. Exacerbated obesogenic response in female mice exposed to early life stress is linked to fat depot-specific upregulation of leptin protein expression. *Am J Physiol Endocrinol Metab*. 2020;319:E852–E862. doi: 10.1152/ajpendo.00243.2020
100. Intapad S, Ojeda NB, Dasinger JH, Alexander BT. Sex differences in the developmental origins of cardiovascular disease. *Physiology (Bethesda)*. 2014;29:122–132. doi: 10.1152/physiol.00045.2013